8-9-2016

# $0^+$ States in $^{130,132}$Xe: A Search for E(5) Behavior

Erin E. Peters
*University of Kentucky*, fe.peters@uky.edu

T. J. Ross
*University of Kentucky*

S. F. Ashley
*University of Kentucky*

Anagha Chakraborty
*University of Kentucky*, anagha@pa.uky.edu

Benjamin P. Crider
*University of Kentucky*, bpscrider@gmail.com

***See next page for additional authors***

**Authors**
Erin E. Peters, T. J. Ross, S. F. Ashley, Anagha Chakraborty, Benjamin P. Crider, M. D. Hennek, Sinong Liu, Marcus T. McEllistrem, Sharmistha Mukhopadhyay, Francisco M. Prados-Estévez, Anthony Paul Ramirez, J. S. Thrasher, and Steven W. Yates

**$0^+$ States in $^{130,132}$Xe: A Search for E(5) Behavior**

**Notes/Citation Information**
Published in *Physical Review C*, v. 94, issue 2, 024313, p. 1-7.



**Digital Object Identifier (DOI)**
https://doi.org/10.1103/PhysRevC.94.024313

# $0^+$ states in $^{130,132}$Xe: A search for E(5) behavior

E. E. Peters,[1] T. J. Ross,[1,2] S. F. Ashley,[1,2] A. Chakraborty,[1,2] B. P. Crider,[2] M. D. Hennek,[3] S. H. Liu,[1,2] M. T. McEllistrem,[2] S. Mukhopadhyay,[1,2] F. M. Prados-Estévez,[1,2] A. P. D. Ramirez,[1,2] J. S. Thrasher,[3,4] and S. W. Yates[1,2]

[1]*Department of Chemistry, University of Kentucky, Lexington, Kentucky 40506-0055, USA*

[2]*Department of Physics & Astronomy, University of Kentucky, Lexington, Kentucky 40506-0055, USA*

[3]*Department of Chemistry, University of Alabama, Tuscaloosa, Alabama 35487, USA*

[4]*Department of Chemistry, Advanced Materials Research Laboratory, Clemson University, Anderson, South Carolina 29625, USA*

(Received 16 May 2016; published 9 August 2016)

The level structures of $^{130,132}$Xe were studied with the inelastic neutron scattering reaction followed by $\gamma$-ray detection. Level lifetimes were measured using the Doppler-shift attenuation method and low-lying excited states in these nuclei were characterized. With a focus on the decay properties of the $0^+$ states, these nuclei were examined as representations of the E(5) critical-point symmetry.

DOI: 10.1103/PhysRevC.94.024313

## I. INTRODUCTION

Some isotopic chains span a region which exhibits a gradual transition in structure. For example, the stable Xe nuclei appear to be $\gamma$-soft rotors for the lighter-mass isotopes, while $^{136}$Xe at a closed neutron shell ($N = 82$) appears more spherical in nature. As shown in Fig. 1, predictable patterns emerge at the closed neutron shell with the energy of the first excited state at a maximum, as well as the ratio $E(4_1^+)/E(2_1^+)$ at a minimum, but otherwise the values exhibit gradual change with neutron number. The maximum in the $B(E2; 2_1^+ \rightarrow 0_1^+)$ value occurs as expected at mid-shell with a minimum at or near the closed shell, but characterizing the transitional region between requires more detailed spectroscopic information. By studying this isotopic chain, the structures of these nuclei should lend insight into the nature of the transition which occurs.

Transitional nuclei have proven difficult to describe with conventional nuclear structure models; however, a possible interpretation is to depict such nuclei as undergoing a phase transition. Iachello [2] proposed that a critical point may exist in such a transition, similar to that exhibited by matter undergoing a phase transition. The E(5) symmetry corresponds to a system undergoing a second-order phase transition. In nuclei, this symmetry may be used to describe the critical point of the transition from a spherical vibrator to a $\gamma$-soft rotor. Within the dynamical symmetries of the interacting boson model (IBM), E(5) represents the critical point between the U(5) and O(6) symmetries. The predictions given in Ref. [2] are only applicable to the infinite-$N$ limit of the IBM, but calculations to obtain E(5) predictions for finite boson number are possible, such as those presented in Ref. [3].

The predictions for the E(5) decay scheme are shown in Fig. 2. The $\xi$ quantum number labels major families, and $\tau$ labels the phonon-like structure within each family. An experimental candidate for an E(5) nucleus, $^{134}$Ba, was proposed by Casten and Zamfir [3]. Although absolute transition probabilities were not available for a full comparison with the calculations, their conclusion was that "$^{134}$Ba is close to exemplifying E(5) symmetry" [3]. To date, no better example of the E(5) critical-point symmetry has emerged.

Clark *et al.* [4] embarked on a systematic pursuit of possible E(5) candidates, and conducted a search through the ENSDF database [1] for nuclei possessing E(5) characteristics. The first level of the search was in mass regions known to contain transitional nuclei, $30 \leqslant Z \leqslant 82$ and $A \geqslant 60$, with $2.00 < E(4_1^+)/E(2_1^+) \leqslant 2.40$, which produced over 70 candidates. The second requirement applied was the existence of two excited $0^+$ states within 2.5 and 4.5 times $E(2_1^+)$. After application of these criteria, only six nuclei remained: $^{102}$Pd, $^{106,108}$Cd, $^{124}$Te, $^{128}$Xe, and $^{134}$Ba. Upon comparing the available data with the remaining criteria concerning the decays of the excited $0^+$ states, only $^{128}$Xe and $^{134}$Ba were deemed viable candidates. As $^{134}$Ba had already been proposed by Casten and Zamfir [3], $^{128}$Xe was the lone surviving new E(5) candidate.

In 2009, Coquard *et al.* [5] reported the results of their study of $^{128}$Xe by Coulomb excitation in inverse kinematics. Detailed spectroscopic information was obtained, including $B(E2)$ values for many transitions. Focusing on the relative energies of the excited $0^+$ states and the absolute $B(E2)$ values for their decays, they concluded that $^{128}$Xe does not embody an E(5) nucleus, and suggested that $^{130}$Xe may rather be a better candidate [5]. However, Coulomb excitation measurements on $^{130,132}$Xe published by the same group did not include an evaluation of the E(5) character of these isotopes [6], presumably because in neither nucleus were the excited $0^+$ states significantly populated.

Inelastic neutron scattering (INS) can be utilized to nonselectively populate low-spin states, and lifetimes can be determined with the Doppler-shift attenuation method (DSAM); i.e., $B(E2)$'s can be determined for non-yrast states. Therefore, the $(n,n'\gamma)$ reaction was used to probe the level structures of $^{130,132}$Xe, and information was obtained in the current work which allowed comparisons of these nuclei with the E(5) predictions.

## II. EXPERIMENTS

As xenon is gaseous under ambient conditions, previous scattering experiments to study the Xe isotopes have required the use of high-pressure gas or cryogenic targets, which create a host of difficulties, or experiments were performed with xenon projectiles in inverse kinematics. For the INS measurements, highly enriched (>99.9%) xenon gas was

 

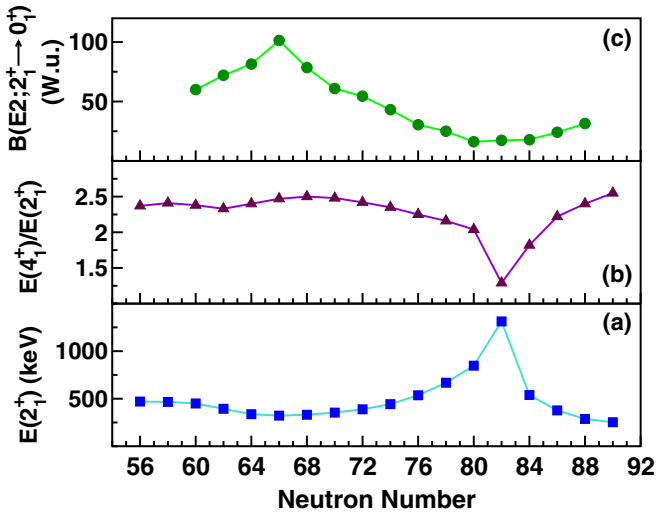


FIG. 1. Properties of the xenon isotopes. Panel (a) shows the energy of the $2_1^+$ state, $E(2_1^+)$, vs neutron number; panel (b) displays $E(4_1^+)/E(2_1^+)$ vs neutron number; and panel (c) exhibits $B(E2; 2_1^+ \rightarrow 0_1^+)$ vs neutron number. Data are taken from Ref. [1].

converted to solid $XeF_2$. $XeF_2$ was prepared by a photochemical [7] or a thermal [8] reaction of $F_2$ and Xe gases in excess Xe; an excess of Xe gas is required in order to ensure only the difluoride is produced rather than the tetrafluoride and hexafluoride as well. From the syntheses, 6.80 g of $^{130}Xe\,F_2$ and 9.89 g of $^{132}Xe\,F_2$ were obtained. Because $XeF_2$ is an excellent fluorinating agent, the samples were placed in polytetrafluoroethylene (PTFE) vials to prevent chemical reactions with their containers. $XeF_2$ is also unstable in air and reactive with moisture, thus the vials were filled under an argon atmosphere, sealed with PTFE tape, and stored in an argon-filled dessicator. To date, this work is the only known implementation of highly enriched solid xenon targets in scattering experiments.

The inelastic neutron scattering, $(n,n'\gamma)$, measurements were performed at the University of Kentucky Accelerator Laboratory (UKAL). Neutrons were produced by bombarding tritium gas with protons from a 7-MV single-stage Van de Graaff accelerator. The resulting nearly monoenergetic neutrons from the $^3H(p,n)^3He$ reaction were scattered from the xenon difluoride samples and the emitted $\gamma$ rays were detected by an ≈50% high-purity germanium (HPGe) detector surrounded by an annular bismuth germanate (BGO) detector for active Compton suppression. The pulsed and bunched proton beam (≈1-ns pulse every 533 ns) allowed time-of-flight gating for further background reduction. A $BF_3$ long counter as well as an NE213 scintillator were used as monitors of the neutron flux for normalization. By varying the incident neutron energy in 100-keV steps and observing the $\gamma$-ray yields, excitation functions were obtained. Angular distribution measurements were performed by varying the detection angle from 40° to 150° with incident neutron energies of 2.0 and 2.5 MeV for $^{130}Xe$, and 2.2 and 2.7 MeV for $^{132}Xe$.

A detailed description of the Doppler-shift attenuation method (DSAM) following inelastic neutron scattering (INS) is given in Ref. [9]. The DSAM-INS measurements rely on careful determinations of $\gamma$-ray energy as a function of detection angle. From this information, the attenuation factor, $F(\tau)$, which describes the deceleration and stopping process of the recoiling nucleus within the material, may be extracted from

$$E_\gamma(\theta) = E_0\left[1 + F(\tau)\frac{v_{c.m.}}{c}\cos\theta\right], \qquad (1)$$

where $E_\gamma(\theta)$ is the $\gamma$-ray energy as a function of the angle of detection with respect to the direction of the incident neutrons, $E_0$ is the energy of the $\gamma$ ray emitted by the nucleus at rest, $v_{c.m.}$ is the center-of-mass velocity of the recoiling nucleus, and $c$ is the speed of light. The $F(\tau)$ values are calculated theoretically as a function of lifetime with the Winterbon formalism [10] describing the stopping process of the recoiling nucleus within

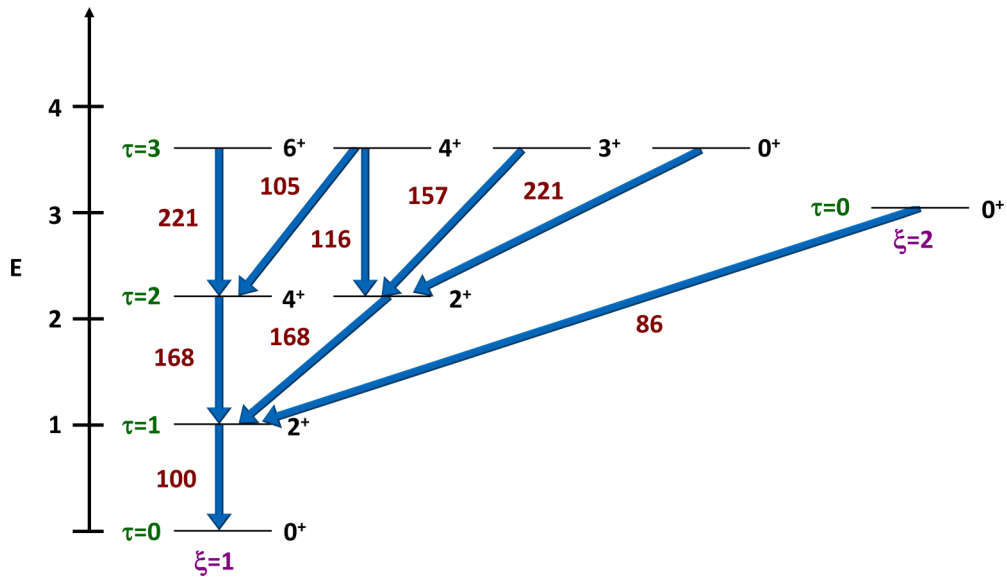


FIG. 2. Lowest portion of the theoretical level scheme for the E(5) critical-point symmetry. Energies are given relative to $E(2_1^+)$ and $B(E2)$'s are given relative to $B(E2; 2_1^+ \rightarrow 0_1^+)$. From Ref. [2].

the material. The recoil energies are on the order of tens of keV, where the nuclear contribution to the stopping power dominates over the electronic component. It is also assumed that Bragg's rule [11] is valid; i.e., the stopping powers for a compound are given by the sum of those for the individual elements in their stoichiometric ratios. From a comparison of the experimental $F(\tau)$ values with the theoretical values, the corresponding lifetimes may be determined.

## III. RESULTS

The data for the levels and transitions pertinent to the E(5) description are given in Tables I and II for $^{130}$Xe and $^{132}$Xe, respectively.

### A. Excited $0^+$ states in $^{130}$Xe

As noted previously [4,5], the lowest excited $0^+$ states play a crucial role in the E(5) picture, so special attention was paid to characterizing these excitations. From thermal neutron capture data, a level at 1590 keV was proposed as the first excited $0^+$ state of $^{130}$Xe by Hamada *et al.* [15]. In the present INS measurements, however, no evidence of the decays of this level was found and we refute its existence.

The $\gamma$ rays from the 1792.8-keV level are observed at the expected energy threshold, and the data are in agreement with the $J^\pi = 0^+$ assignment. The strength of the 670.6-keV transition plays a large role in the description of $^{130}$Xe as an

TABLE I. Levels, transitions, initial spins and parities, final spins and parities, branching ratios, average experimental attenuation factors, lifetimes, multipole mixing ratios, and reduced transition probabilities for $^{130}$Xe. Energies are in keV, lifetimes are in fs, and $B(E2)$ values are in W.u.

| $E_{\text{level}}$ | $E_\gamma$ | $J_i^\pi$ | $J_f^\pi$ | B.R. | $\bar{F}(\tau)$ | $\tau$ | $\delta$ | $B(E2)$ |
|---|---|---|---|---|---|---|---|---|
| 536.068(6)[a] | 536.066(6)[a] | $2_1^+$ | $0_1^+$ | 1 | | 14200(1100)[b] | $E2$ | 33.2(26)[b] |
| 1122.14(2) | 586.07(1) | $2_2^+$ | $2_1^+$ | 0.858(4) | | 6100(1100)[c] | $4.41^{+42}_{-51}$ | $40^{+10}_{-7}$ |
| | | | | | | | $-0.160^{+18}_{-15}$ | $1.06^{+49}_{-35}$ |
| | 1122.13(5) | | $0_1^+$ | 0.142(4) | | | $E2$ | $0.27^{+7}_{-5}$ |
| 1204.66(2) | 668.59(1) | $4_1^+$ | $2_1^+$ | 1 | | 3380(340)[c] | $E2$ | 46.4(46)[d] |
| 1632.62(3) | 427.96(3) | $3_1^+$ | $4_1^+$ | 0.056(7)[a] | 0.049(32) | $1300^{+2500}_{-600}$ [e] | $3.0^{+15}_{-10}$ | $57^{+59}_{-42}$ |
| | | | | | | | $0.51^{+17}_{-13}$ | $13^{+25}_{-11}$ |
| | 510.51(10) | | $2_2^+$ | 0.572(28)[a] | | | | $\leqslant 270$[f] |
| | 1096.64(10)[e] | | $2_1^+$ | 0.372(20)[a] | | | $0.611^{+46}_{-41}$ [e] | $1.0^{+10}_{-7}$ |
| 1792.75(6) | 670.6(1) | $0_2^+$ | $2_2^+$ | 0.216(44)[g] | 0.187(84)[h] | $290^{+290}_{-110}$ [h] | $E2$ | $120^{+110}_{-70}$ |
| | 1256.7(1)[h] | | $2_1^+$ | 0.78(16)[g] | | | $E2$ | $18^{+17}_{-11}$ |
| 1808.22(2) | 603.55(4) | $4_2^+$ | $4_1^+$ | 0.184(6) | 0.067(54) | $980^{+4430}_{-460}$ | $2.4^{+13}_{-7}$ | $42^{+48}_{-35}$ |
| | | | | | | | $-0.37^{+18}_{-20}$ | $6^{+18}_{-6}$ |
| | 686.09(2) | | $2_2^+$ | 0.491(7) | | | $E2$ | $69^{+65}_{-57}$ |
| | 1272.15(5) | | $2_1^+$ | 0.324(7) | | | $E2$ | $2.1^{+20}_{-17}$ |
| 1944.140(12)[a,i] | 739.512(10)[a] | $6_1^+$ [a] | $4_1^+$ | 1 | | 1370(180)[c] | $E2$ | 69(9)[d] |
| 2016.22(10) | 894.08(10) | $0_3^+$ | $2_2^+$ | 1 | 0.094(54) | $670^{+980}_{-270}$ | $E2$ | $55^{+37}_{-33}$ |
| 2017.91(3) | 1481.84(2)[j] | $2^+$ | $2_1^+$ | 0.974(9)[k] | 0.154(36) | $380^{+140}_{-90}$ [j] | $2.95^{+30}_{-31}$ | $6.7^{+22}_{-19}$ |
| | | | | | | | $-0.068^{+37}_{-42}$ | $0.034^{+81}_{-29}$ |
| | 2017.8(2)[k] | | $0_1^+$ | 0.026(9)[k] | | | $E2$ | $0.043^{+31}_{-22}$ |

[a]From Ref. [12].
[b]From Ref. [13].
[c]Calculated using data in Ref. [6].
[d]From Ref. [6].
[e]Determined from the 1096.6-keV $\gamma$ ray, which has a contaminant from a known background $\gamma$ ray which does not exhibit a Doppler shift.
[f]Only upper limits could be determined due to contamination of the 510.5-keV $\gamma$ ray from the 511-keV annihilation radiation. This value was calculated assuming pure $E2$ multipolarity.
[g]The branching ratios for the 1256.7-keV and 670.6-keV $\gamma$ rays were determined from the 102° spectrum where the contaminations from a $\gamma$ ray from $^{19}$F at angles $>102°$ for the 1256.7-keV $\gamma$ ray and from a known background $\gamma$ ray from $^{63}$Cu$(n,n'\gamma)$ at angles $\leqslant 90°$ for the 670.6-keV $\gamma$ ray were minimized.
[h]Determined using only the 1256.7-keV $\gamma$ ray at angles $\leqslant 102°$ due to contaminations described in footnote [g] above.
[i]Information for this level could not be obtained from the current measurements due to contamination of the 739.5-keV $\gamma$ ray from a known $^{72}$Ge$(n,\gamma)^{73}$Ge background $\gamma$ ray.
[j]Determined using only the 1481.8-keV $\gamma$ ray at angles $\geqslant 90°$ due to contamination from a known background $\gamma$ ray from $^{65}$Cu$(n,n'\gamma)$ at forward angles and the 2017.8-keV $\gamma$ ray being too weak to measure the angular distribution.
[k]Determined by summing all of the angles $\geqslant 90°$ in the 2.5-MeV angular distribution as the 2017.8-keV $\gamma$ ray is not observed in the single-angle spectra and the 1481.8-keV $\gamma$ ray is contaminated at angles $<90°$.

TABLE II. Levels, transitions, initial spins and parities, final spins and parities, branching ratios, average experimental attenuation factors, lifetimes, multipole mixing ratios, and reduced transition probabilities for $^{132}$Xe. Energies are in keV, lifetimes are in fs, and $B(E2)$ values are in W.u.

| $E_{\text{level}}$ | $E_\gamma$ | $J_i^\pi$ | $J_f^\pi$ | B.R. | $\bar{F}(\tau)$ | $\tau$ | $\delta$ | $B(E2)$ |
|---|---|---|---|---|---|---|---|---|
| 667.715(2)[a] | 667.714(2)[a] | $2_1^+$ | $0_1^+$ | 1 | | 6680(440)[b] | $E2$ | 23.0(15)[b] |
| 1297.95(2) | 630.23(1) | $2_2^+$ | $2_1^+$ | 0.944(2) | | 4400(620)[a] | $3.15^{+30}_{-22}$ | $40.1^{+74}_{-55}$ |
| | 1298.02(3) | | $0_1^+$ | 0.056(2) | | | $E2$ | |
| 1440.37(2) | 772.65(1) | $4_1^+$ | $2_1^+$ | 1 | | 2600(200)[a] | $E2$ | 28.6(23)[a] |
| 1803.81(2) | 363.44(5) | $3_1^+$ | $4_1^+$ | 0.048(3) | | >10000 | $0.7^{+23}_{-2}$ | <5 |
| | | | | | | | $2.0^{+10}_{-16}$ | <13 |
| | 505.87(2) | | $2_2^+$ | 0.574(14) | | | $4.44^{+39}_{-55}$ | <34 |
| | 1136.07(2) | | $2_1^+$ | 0.378(13) | | | $0.459^{+51}_{-45}$ | <0.07 |
| 1948.20(4) | 1280.48(3) | $0_2^+$ | $2_1^+$ | 1 | 0.044(32) | $1500^{+3900}_{-700}$ | $E2$ | $4.0^{+31}_{-29}$ |
| 1962.98(3) | 522.60(2) | $4_2^+$ | $4_1^+$ | 0.879(6) | 0.047(24) | $1500^{+1500}_{-500}$ | $-0.214^{+23}_{-26}$ | $14^{+12}_{-8}$ |
| | 1295.62(10) | | $2_1^+$ | 0.121(6) | | | $E2$ | $0.45^{+26}_{-24}$ |
| 2167.35(8) | 726.98(5) | $(6^+)$ | $4_1^+$ | 1 | 0.089(80) | $700^{+6900}_{-400}$ | $E2$ | $140^{+190}_{-130}$ |
| 2169.25(5) | 1501.53(3) | $0_3^+$ | $2_1^+$ | 1 | 0.244(27) | $225^{+36}_{-30}$ | $E2$ | $11.9^{+18}_{-16}$ |

[a]From Ref. [14].
[b]From Ref. [13].

E(5) nucleus. The branchings for the two $\gamma$ rays from this level have been previously determined only by Hopke *et al.* from $\beta$ decay [16]; however, the uncertainties are large, i.e., 0.14(7) and 0.86(17) for the 670.6- and 1256.7-keV branches, respectively. A recent study of $^{130}$Cs decay was performed by Betterman *et al.* [17], but unfortunately, they did not report values for these branchings.

In order to determine the strength of the 670.6-keV transition, the lifetime of the 1792.8-keV level and the branching ratio of the $0_2^+ \rightarrow 2_1^+$ transition must be determined. The measurement of each of these quantities suffers some difficulties in our experiments. As the 670.6-keV $\gamma$ ray is in the tail of the 668.6-keV $\gamma$ ray from the $4_1^+ \rightarrow 2_1^+$ transition, which is much more intense at all incident neutron energies, determining the intensity of this $\gamma$ ray is difficult. To address this problem, we measured spectra with 2.0-MeV neutrons and with 1.7-MeV neutrons. At the lower energy, which is below the threshold for population of the 1792.8-keV level, only the 668.6-keV $\gamma$ ray is observed and the peak-fitting parameters for this $\gamma$ ray can be determined for analysis of the doublet in the spectrum taken at the higher energy. In addition, the scaled 668.6-keV $\gamma$ ray could be subtracted from the higher-energy spectrum so that only the 670.6-keV $\gamma$ ray remained. Both approaches provided $\gamma$-ray intensities in good agreement.

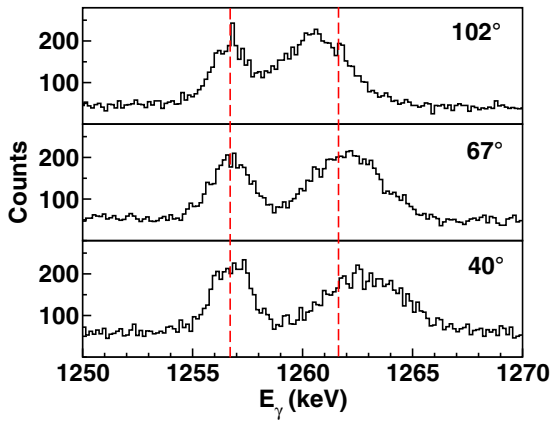


FIG. 3. Spectra from the 2.0-MeV angular distribution at three angles for $^{130}$Xe. The 1256.7-keV $\gamma$ ray is obscured by a Doppler-broadened 1261.6-keV $\gamma$ ray from $^{19}$F at angles >102°.

The 1256.7-keV $\gamma$ ray from the $0_2^+ \rightarrow 2_1^+$ transition was used to determine the lifetime of the $0_2^+$ level, but it is adjacent to a 1261.6-keV Doppler-broadened peak from $^{19}$F, which is present in the scattering sample as well as the PTFE container. At forward angles, these $\gamma$ rays are resolved, but at backward angles the peak from $^{19}$F moves over the 1256.7-keV $\gamma$ ray (see Fig. 3). Lifetime determinations were performed at incident neutron energies of 2.0 and 2.5 MeV, with the lower energy providing more reliable data. Useful spectra for the lifetime determination were obtained at angles between 40° and 102° (see Fig. 4); however, the lifetime obtained exhibits large uncertainties, as does the $B(E2)$ value.

The assignment of the 2016-keV level in $^{130}$Xe has been the source of considerable confusion. The $0^+$ spin assignment originated from the observation of an $E0$ transition from the level to the ground state following the $\beta$ decay of $^{130}$Cs [18]. Additional evidence supporting this assignment can be found in the recently published $^{132}$Xe$(p,t)^{130}$Xe reaction data, showing population of an $l = 0$ state at 2017 keV [19]. Complexity in this assignment arises, however, from two other measurements. Data from the $^{128}$Te$(^3$He$,n)^{130}$Xe transfer reaction indicated that both $l = 0$ and $l = 2$ states occur at an energy of $2.13 \pm 0.10$ MeV [20]. In addition, it was concluded from recent Coulomb excitation measurements that the level is a $2^+$ state, based on the observation of a $\gamma$ ray to the ground state [6]. In the present experiments, we distinctly observe two separate levels: a $0^+$ state at 2016.2 keV and a $2^+$ state at 2017.9 keV. The angular

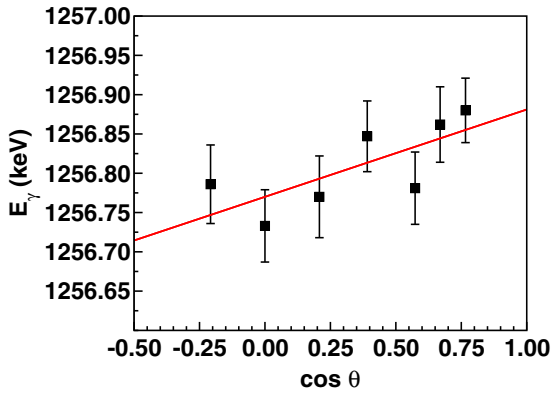


FIG. 4. Doppler-shift of the 1256.7-keV $\gamma$ ray from $^{130}$Xe. The experimental $F(\tau)$ value is 0.187(84), which corresponds to a lifetime of $290^{+290}_{-110}$ fs.

distribution of the 1481.8-keV $\gamma$ ray is anisotropic as shown in Fig. 5, and it thus cannot originate from a spin-0 state. The angular distribution of the 894.1-keV $\gamma$ ray is isotropic, however, and the measured $\gamma$-ray energies result in level energies that differ by 1.7 keV. We also observe a $\gamma$ ray to the ground state, whose energy is in agreement with the 2017.9-keV level. A comparison of the relative $\gamma$-ray cross section as a function of incident neutron energy with statistical model calculations using the code CINDY provides additional evidence for assigning two separate levels with $J^\pi = 0^+$ and $2^+$, as shown in Figs. 6 and 7.

### B. Excited $0^+$ states in $^{132}$Xe

The 1948.2-keV level has been identified only in this work, and a single 1280.5-keV $\gamma$ ray corresponding to a transition to the $2^+_1$ state is placed. The isotropic angular distribution of this $\gamma$ ray suggests a spin assignment of $J^\pi = 0^+$. A comparison of the relative $\gamma$-ray cross section as a function of incident neutron energy with statistical model calculations using the code CINDY confirms this spin assignment.

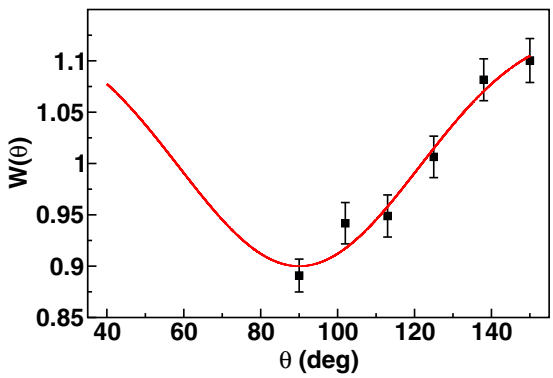


FIG. 5. Angular distribution of the 1481.8-keV $\gamma$ ray from the 2017.9-keV level in $^{130}$Xe. The 1481.8-keV $\gamma$ ray is contaminated by a $\gamma$ ray from $^{65}$Cu background at angles $<90^\circ$, thus those data were not included in the analysis.

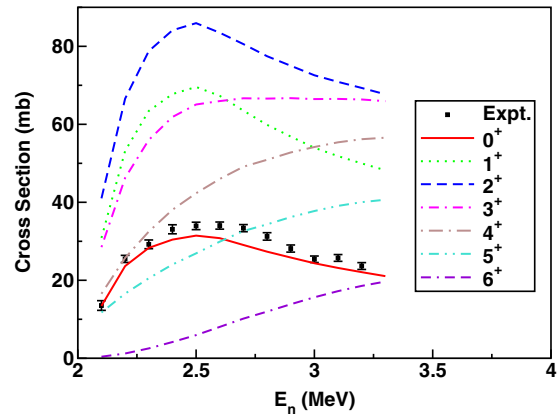


FIG. 6. Relative experimental cross section compared with statistical model calculations for the 2016.2-keV level in $^{130}$Xe. The data agree well with the calculation for $J^\pi = 0^+$.

The 2169.2-keV level was previously assigned a spin-parity of 1 or $2^+$ [21]. We find evidence for only one of the reported $\gamma$ rays from this level: the 1501.5-keV $\gamma$ ray to the $2^+_1$ state, which has an isotropic angular distribution. When compared with the CINDY calculations, the excitation function does not agree with a spin of 1 or $2^+$, but rather supports $0^+$. A ground-state $\gamma$ ray observed in neutron capture at thermal energies and at a resonant energy of 14.1 eV [15,21] is reported in the NDS [14], but no primary $\gamma$ ray was observed to this level, and it was only assumed that the 2169-keV $\gamma$ ray represented a transition to the ground state. This $\gamma$ ray is not observed in our measurements.

## IV. DISCUSSION

It has been noted [4,5,22] that the relative positions of the lowest excited $0^+$ states and their absolute $B(E2)$ values are the most sensitive features of the E(5) symmetry. In fact, the arguments by Coquard *et al.* [5] against $^{128}$Xe as an E(5) candidate were based primarily on relative energies and the decay properties of the first two excited $0^+$ states. From the new information on excited $0^+$ states obtained in this work,

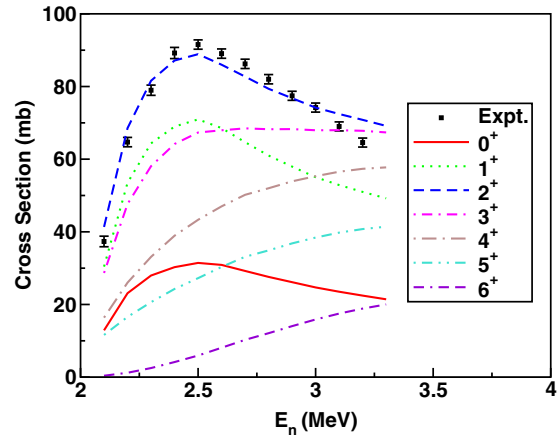


FIG. 7. Relative experimental cross section compared with statistical model calculations for the 2017.9-keV level in $^{130}$Xe. The data agree well with the calculation for $J^\pi = 2^+$.

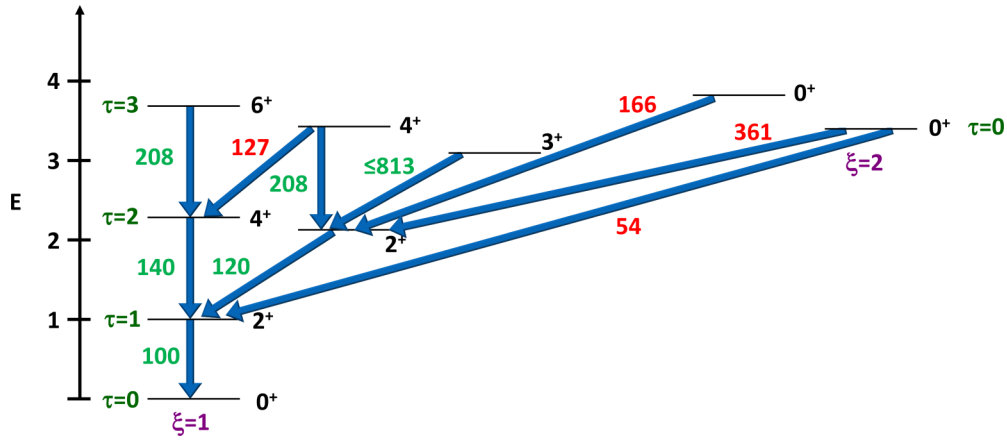


FIG. 8. Lowest portion of the level scheme for $^{130}$Xe in the same format as Fig. 2. Energies are given relative to $E(2_1^+)$ and $B(E2)$'s are given relative to $B(E2; 2_1^+ \rightarrow 0_1^+)$. Values in red were measured for the first time in this work.

comparisons of the structures of $^{130,132}$Xe can be drawn with the predictions of E(5) critical-point symmetry.

In the E(5) picture [2], the $\xi$ quantum number labels major families, and $\tau$ labels the phonon-like structure within each family. The first excited $0^+$ state is predicted to have $\xi = 2$ and $\tau = 0$ (frequently labeled as $0_\xi^+$) and exhibits an allowed decay to the $2_1^+$ level, according to the $\Delta\tau = \pm 1$ selection rule for the $E2$ operator [2,22]. The second excited $0^+$ state is predicted to arise as a three-phonon ($\tau = 3$) state within the $\xi = 1$ family (labeled as $0_\tau^+$) with its allowed decay to the $2_2^+$ level. The evolution of these $0^+$ states across the stable Xe isotopes has been examined by Bonatsos *et al.* [22] and by Coquard *et al.* [5].

As shown in Fig. 2, the $0_2^+$ state should decay only to the $2_1^+$ state and the $0_3^+$ state should decay only to the $2_2^+$ state. In $^{132}$Xe, both the $0_2^+$ and the $0_3^+$ states decay only to the $2_1^+$ state (see Table II), thus eliminating this nucleus from consideration as a representation of the E(5) symmetry. In the case of $^{130}$Xe, however, the allowed decays are observed as shown in Fig. 8. A failing of the comparison, however, is the observation of the forbidden $0_2^+ \rightarrow 2_2^+$ transition with a large $B(E2)$ value, $120^{+110}_{-70}$ W.u., where the large uncertainty of this value arises primarily from the uncertainty of the lifetime. As described in the previous section, we recognized the difficulties in obtaining these values and performed additional measurements to minimize the uncertainties. The formalism introduced by Arias [23] allows for a weak decay from the $0_2^+$ state to the $2_2^+$ state, but the observed decay strength is significantly larger.

The structure of $^{134}$Ba was also compared with E(5) predictions from an IBM calculation for $N = 5$ bosons [3]. This calculation reverses the energy order of the excited $0^+$ states, such that the $0_3^+$ state decays to the $2_1^+$ state and the $0_2^+$ state decays to the $2_2^+$ state, as is evident for $^{134}$Ba. For $^{130}$Xe, $N = 5$ is also appropriate, yet the reversal of the states is not observed.

Further problems with the E(5) comparison arise when examining transfer reaction data. We noted earlier that the 2017-keV $0^+$ state in $^{130}$Xe is populated strongly in the ($^3$He,$n$) two-proton transfer reaction [20] with 39% of the population of the ground state, indicating that this state has a complex structure. Similar $0^+$ states have been observed in the lighter even-mass Xe isotopes [24] and have been interpreted as the main fragment of the proton pairing vibrational band. We do not observe $2^+$ states which feed these $0^+$ states to identify such structures in $^{130,132}$Xe, but these $\gamma$ rays would be low-energy, weak branches and would be difficult to observe in our INS measurements.

## V. CONCLUSIONS

Based on new information garnered from inelastic neutron scattering data, $^{130}$Xe and $^{132}$Xe have been examined as possible representations of the E(5) critical-point symmetry, using the properties of the first and second excited $0^+$ states as the basis for evaluation. In neither case are the expectations of the E(5) symmetry fully realized; decays that are forbidden in the E(5) description are observed in both nuclei. While $^{130}$Xe had been proposed as the remaining "best" candidate for the E(5) symmetry among the xenon isotopes [5], the additional information obtained in the INS studies reveals that this is not the case. It appears that none of the xenon isotopes are clear-cut representations of an E(5) critical-point nucleus.

## ACKNOWLEDGMENTS

This material is based upon work supported by the U.S. National Science Foundation under Grant No. PHY-1305801. We wish to thank H. E. Baber for his invaluable contributions to maintaining the UKAL.

[1] ENSDF, Evaluated Nuclear Structure Data File, a computer file of evaluated nuclear data maintained by the National Nuclear Data Center, Brookhaven National Laboratory, as of April 2014, http://www.nndc.bnl.gov/ensdf/.

[2] F. Iachello, Phys. Rev. Lett. **85**, 3580 (2000).

[3] R. F. Casten and N. V. Zamfir, Phys. Rev. Lett. **85**, 3584 (2000).

[4] R. M. Clark, M. Cromaz, M. A. Deleplanque, M. Descovich, R. M. Diamond, P. Fallon, I. Y. Lee, A. O. Macchiavelli, H. Mahmud, E. Rodriguez-Vieitez, F. S. Stephens, and D. Ward, Phys. Rev. C **69**, 064322 (2004).

[5] L. Coquard, N. Pietralla, T. Ahn, G. Rainovski, L. Bettermann, M. P. Carpenter, R. V. F. Janssens, J. Leske, C. J. Lister, O. Möller, W. Rother, V. Werner, and S. Zhu, Phys. Rev. C **80**, 061304 (2009).
[6] L. Coquard, N. Pietralla, G. Rainovski, T. Ahn, L. Bettermann, M. P. Carpenter, R. V. F. Janssens, J. Leske, C. J. Lister, O. Möller, W. Rother, V. Werner, and S. Zhu, Phys. Rev. C **82**, 024317 (2010).
[7] A. Šmalc, K. Lutar, and S. A. Kinkead, Inorg. Synth. **29**, 1 (1992).
[8] W. E. Falconer and W. A. Sunder, J. Inorg. Nucl. Chem. **29**, 1380 (1967).
[9] T. Belgya, G. Molnár, and S. W. Yates, Nucl. Phys. A **607**, 43 (1996).
[10] K. B. Winterbon, Nucl. Phys. A **246**, 293 (1975).
[11] W. H. Bragg and R. Kleeman, Philos. Mag. **10**, 318 (1905).
[12] B. Singh, Nucl. Data Sheets **93**, 33 (2001).
[13] S. Raman, C. W. Nestor, Jr., and P. Tikkanen, At. Data Nucl. Data Tables **78**, 1 (2001).
[14] Y. Khazov, A. A. Rodionov, S. Sakharov, and B. Singh, Nucl. Data Sheets **104**, 497 (2005).
[15] S. A. Hamada, W. D. Hamilton, and B. More, J. Phys. G: Nucl. Part. Phys. **14**, 1237 (1988).
[16] P. K. Hopke, A. G. Jones, W. B. Walters, A. Prindle, and R. A. Meyer, Phys. Rev. C **8**, 745 (1973).
[17] L. Bettermann, C. Fransen, S. Heinze, J. Jolie, A. Linnemann, D. Mücher, W. Rother, T. Ahn, A. Costin, N. Pietralla, and Y. Luo, Phys. Rev. C **79**, 034315 (2009).
[18] S. A. Bakiev, K. A. Baskova, S. S. Vasil'ev, M. A. Mokhsen, A. A. Sorokin, and T. V. Chugaĭ, Yad. Fiz. **18**, 233 (1973).
[19] B. P. Kay, T. Bloxham, S. A. McAllister, J. A. Clark, C. M. Deibel, S. J. Freedman, S. J. Freeman, K. Han, A. M. Howard, A. J. Mitchell, P. D. Parker, J. P. Schiffer, D. K. Sharp, and J. S. Thomas, Phys. Rev. C **87**, 011302 (2013).
[20] W. P. Alford, R. E. Anderson, P. A. Batay-Csorba, R. A. Emigh, D. A. Lind, P. A. Smith, and C. D. Zafiratos, Nucl. Phys. A **323**, 339 (1979).
[21] W. Gelletly, W. R. Kane, and D. R. MacKenzie, Phys. Rev. C **3**, 1678 (1971).
[22] D. Bonatsos, D. Lenis, N. Pietralla, and P. A. Terziev, Phys. Rev. C **74**, 044306 (2006).
[23] J. M. Arias, Phys. Rev. C **63**, 034308 (2001).
[24] A. J. Radich, P. E. Garrett, J. M. Allmond, C. Andreoiu, G. C. Ball, L. Bianco, V. Bildstein, S. Chagnon-Lessard, D. S. Cross, G. A. Demand, A. Diaz Varela, R. Dunlop, P. Finlay, A. B. Garnsworthy, G. Hackman, B. Hadinia, B. Jigmeddorj, A. T. Laffoley, K. G. Leach, J. Michetti-Wilson, J. N. Orce, M. M. Rajabali, E. T. Rand, K. Starosta, C. S. Sumithrarachchi, C. E. Svensson, S. Triambak, Z. M. Wang, J. L. Wood, J. Wong, S. J. Williams, and S. W. Yates, Phys. Rev. C **91**, 044320 (2015).